5.3 THz MgB2 hot electron bolometer mixer operated at 20 K

Gao, J.R.; Gan, Y.; Mirzaei, B.; Silva, J. R.G.; Cherednichenko, S.

DOI
10.1117/12.2630161

Publication date
2022

Document Version
Final published version

Published in
Millimeter, Submillimeter, and Far-Infrared Detectors and Instrumentation for Astronomy XI

PROCEEDINGS OF SPIE

SPIEDigitalLibrary.org/conference-proceedings-of-spie

5.3 THz MgB2 hot electron bolometer mixer operated at 20 K

J. R. Gao, Y. Gan, B. Mirzaei, J. R.G. Silva, S. Cherednichenko

J. R. Gao, Y. Gan, B. Mirzaei, J. R.G. Silva, S. Cherednichenko, "5.3 THz MgB2 hot electron bolometer mixer operated at 20 K," Proc. SPIE 12190, Millimeter, Submillimeter, and Far-Infrared Detectors and Instrumentation for Astronomy XI, 121900F (31 August 2022); doi: 10.1117/12.2630161

SPIE.

Event: SPIE Astronomical Telescopes + Instrumentation, 2022, Montréal, Québec, Canada

5.3 THz MgB_2 hot electron bolometer mixer operated at 20 K

J.R. Gao[a,b,*], Y. Gan[a,c], B. Mirzaei[a,b], J.R.G. Silva[a,c], S. Cherednichenko[d]
[a]*SRON Netherlands Institute for Space Research, Niels Bohrweg 4, 2333 CA Leiden, and Landleven 12, 9747 AD Groningen, the Netherlands*
[b]*Optics Research Group, Department of Imaging Physics, Delft University of Technology, Delft, 2628 CJ, the Netherlands*
[c]*Kapteyn Astronomical Institute, University of Groningen, Groningen, 9747 AD, the Netherlands*
[d]*Terahertz and Millimetre Wave Laboratory, Department of Microtechnology and Nanoscience, Chalmers University of Technology, SE-412 96 Gothenburg, Sweden*

ABSTRACT

Heterodyne receivers combining a NbN HEB mixer with a local oscillator (LO) are the work horse for high resolution ($\geq 10^6$) spectroscopic observations at supra-terahertz frequencies. We report an MgB_2 HEB mixer working at 5.3 THz with 20 K operation temperature based on a previously published paper [Y. Gan *et al*, Appl. Phys. Lett., **119**, 202601 (2021)]. The HEB consists of a 7 nm thick MgB_2 submicron-bridge contacted with a spiral antenna. It has a T_c of 38.4 K. By using hot/cold blackbody loads and a Mylar beam splitter all in vacuum, and applying a 5.25 THz FIR gas laser as the LO, we measured a minimal DSB *receiver* noise temperature of 3960 K. The latter gives a DSB *mixer* noise temperature of 1470 K. This sensitivity is 28 times better than a room temperature Schottky mixer at 4.7 THz, but about 2.5 times less sensitive than an NbN HEB mixer. The latter must be operated around 4 K. The IF noise bandwidth is about 10 GHz, which is 2.5-3 times larger than an NbN HEB. With further optimization, such MgB_2 HEBs are expected to reach a better sensitivity. That the low noise, wide IF bandwidth MgB_2 HEB mixers can be operated in a compact, low dissipation 20 K Stirling cooler can significantly reduce the cost and complexity of heterodyne instruments and therefore facilitate new space missions.

Keywords: Hot electron bolometer, mixer, THz, MgB_2, superconductor, high Tc, IF bandwidth, space instrumentation

1. INTRODUCTION

Superconducting hot electron bolometer (HEB) mixers [1] are so far the most sensitive heterodyne detectors for high-resolution spectroscopy at the supra-THz frequencies between 1 and 6 THz [2]. They play a key role in astrophysics in this frequency region, as this region is rich in the atomic, ionic, and molecular spectral lines that can, for example, directly probe how star formation proceeds in galaxies [3]. Such mixers have been successfully applied for the airborne telescope of Stratospheric Observatory for Infrared Astronomy [4], the balloon-borne telescope of Stratospheric Terahertz Observatory 2 [5], and the space telescope of the Herschel Space Observatory [6].

To date, HEB mixers based on thin NbN films have shown excellent sensitivities where their best double sideband (DSB) receiver noise temperature (T_{rec}^{DSB}) is approaching seven times the quantum noise (QN) at the high end of supra-THz frequencies [7], while a DSB mixer noise temperature (T_m^{DSB}) is approaching only four times QN [8]. The QN is characterized by hν/2k for the case of single side band, corresponding to 48 k/THz, where *h* is the Planck constant, ν the frequency, and k the Boltzmann constant. However, one drawback of such mixers is their limited intermediate frequency (IF) bandwidth, typically 3-4 GHz. Another drawback comes from the low operating temperature around 4 K due to their low critical temperature (T_c) of 8-10 K. Cooling down to 4 K, either by using Liquid He vessels or a mechanical pulse tube, is suboptimal for a space observatory considering the constraints on mass, volume, electrical power, and, in particular, cost in practice. For example, for the next generation of THz observatories with a number of telescopes operated as an interferometer in space [9] and the Earth atmospheric observations from space [10], the weight and consumed electrical power of cryo-coolers becomes much less if the operating temperature could be tolerated to 20 K or above.

*j.r.gao@sron.nl; j.r.gao@tudelft.nl

Millimeter, Submillimeter, and Far-Infrared Detectors and Instrumentation for Astronomy XI, edited by Jonas Zmuidzinas, Jian-Rong Gao, Proc. of SPIE Vol. 12190, 121900F · © 2022 SPIE · 0277-786X · doi: 10.1117/12.2630161

Superconducting MgB_2 with a T_c of 40 K in bulk [11] is considered as a candidate to increase the IF bandwidth of an HEB mixer and also the operating temperature. The first MgB_2 HEB mixer based on a Molecular Beam Epitaxy (MBE) growth, 20 nm thick film with a T_c of 22 K was reported at 1.6 THz [12]. The HEB mixers based on Hybrid Physical Chemical Vapor Deposition (HPCVD) growth MgB_2 films, 10-20 nm, with an increased T_c of 33-38 K were reported at 600 GHz [13]. An HEB mixer based on a MgB_2 film of 7 nm with a T_c of 34 K, milled from a thicker film by an Ar ion mill, was measured at 600 GHz and 1.9 THz, with a T_{rec}^{DSB} of 3600 K at 1.9 THz and an IF noise bandwidth (NBW) of 6.5 GHz [14]. A combination of both a low T_{rec}^{DSB} of 930 K at 1.6 THz and a high NBW of 11 GHz in an MgB_2 HEB mixer at 5 K was reported in [15], which was based on an HPCVD, 5 nm film with a T_c of 31 K. The T_{rec}^{DSB} of this mixer increases by 75 % at 20 K. A similar T_{rec}^{DSB} (1000 K) at 1.6 THz together with a NBW of 13 GHz was achieved in [16]. The results in [14-16] raise the interesting question of whether it is suitable for the operation at 20 K, a temperature which is attractive for space applications because of the availability of the compact, low mass, low dissipation, and space qualified Stirling coolers [17].

MgB_2 HEB mixers are thus the alternative to detect, for example, the astrophysically important neutral atomic oxygen [OI] line at 4.75 THz and molecular Hydrogen deuteride HD(2-1) line at 5.33 THz, which can only be observed from space and which usually require an IF bandwidth of ≥4 GHz. The latter is a bit beyond the capability of the NbN technology. However, until now, no sensitivity of such mixers has been reported at the frequencies above 1.9 THz in the literature although some measurements up to 4.3 THz have been reported in [18].

In this conference paper, we summarize the results of an MgB_2 HEB mixer operated at 5.3 THz, which is the highest frequency studied so far. The key results and their analysis have been published earlier in [19]. We repeat them here, but update the discussions and add necessary details of the HEB fabrication and test setup. In essence, we increase the T_c of the MgB_2 film to 38.4 K [20] by increasing the thickness from 5 nm in [15] to 7 nm, i.e. close to its maximum theoretical value. The MgB_2 HEBs were fabricated as submicron-bridges integrated with a spiral antenna. Our experiment focuses at T_{rec}^{DSB} at 20 K. But we also studied the T_{rec}^{DSB}, T_m^{DSB}, conversion gain (G_m^{DSB}), and output noise (T_{out}) from 6 K up to 23 K in order to fully characterize such a new mixer. In addition, the IF noise bandwidth was measured in the frequency range between 0.2-14 GHz to characterize it directly at 5.3 THz LO and 20 K.

2. HEB AND MEASUREMENT SETUP

2.1 MgB_2 HEB and fabrication

The HEB used (#MgB2_BM3_2b), as shown in the inset (a) of Figure 2, consists of a 285 nm wide, 850 nm long, and 7 nm thick MgB_2 bridge on a 0.32 mm thick SiC substrate. The narrow bridge is to minimize the HEB volume and hence to reduce the required LO power. So, it can be operated with an existing FIR gas laser in the lab. The bridge is connected to a planar spiral antenna consisting of a 195 nm thick Au layer through contact-pads made of an Au layer with a thickness of ≥ 60 nm. The taped contact-pads are designed to reduce the reactance [21]. The antenna is designed to match the HEB impedance of 80 Ω with an upper cutoff frequency of ≥ 6 THz [22].

The HEB devices were realized as a collaboration between two labs. The MgB_2 film was grown by the HPCVD at Chalmers University of Technology, Sweden. The film is 7 nm thick according to the growth rate and deposition time. To minimize oxidation, the film, when taken out from the HPCVD chamber after the growth, is immediately loaded into a sputter machine, where an in-situ Au (20 nm) deposition is performed on the top of the MgB_2 film after a sputter cleaning.

MgB_2 HEB devices were fabricated at Delft University of Technology, the Netherlands. The fabrication starts with the definition of the contact-pads with e-beam lithography (EBL) and Au evaporation in combination with a lift-off process. Then, the spiral antennas are defined using a similar process, but by evaporating a thicker Au layer together with a layer of Ti on the top. The latter is to prevent etching of the Au antenna during the Ar Ion beam milling etching (IBME) to define the MgB_2 bridge width. Now, the Au layer of 20 nm (protecting the MgB_2) is removed using IBME, followed immediately by depositing a layer of Si_3N_4 (80 nm) in a sputter machine to avoid the oxidation of MgB_2 through the rest of the process. The etching mask to define the submicron-bridges is then patterned using EBL. Finally, the uncovered Si_3N_4 and MgB_2 are etched away using IBME to form MgB_2 bridges. Before dicing the wafer to HEB chips, a thick layer of Si_3N_4 is sputtered to cover the surface of the chips except for the bonding pads to isolate MgB_2 bridges from water and air.

The HEB used has a room temperature resistance of 92 Ω and has a normal-state resistance of 51 Ω measured at above its T_c. (defined by the films sheet resistance and the bridge aspect ratio), which is also the impedance at 5.3 THz

[23]. The HEB has a T_c of 38.4 K and a critical current of 1.3 mA at 5 K, corresponding to a current density of 6.5×10^7 A/cm^2, which is a factor of 3 higher than what was reported in [15].

2.2 Measurement setup

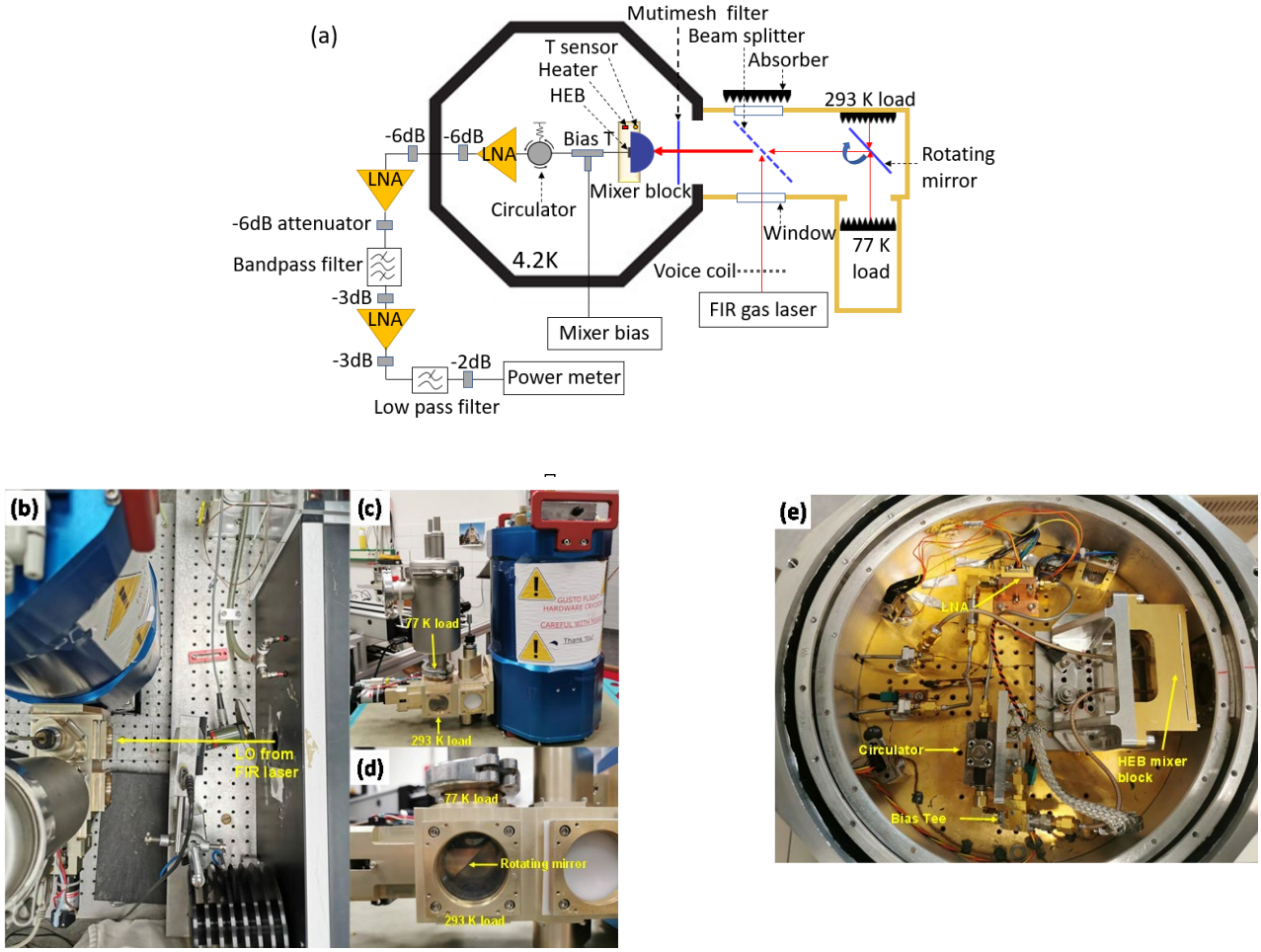

FIG. 1. Schematics of the measurement setup for measuring the and at 1.7 GHz in (a). The hot/cold loads and the Mylar beam splitter are placed in a vacuum enclosure, attached to the cryostat. A rotating mirror is used to switch between hot and cold loads. The (5.8 THz) low pass filter functions as a heat filter, Three photo views (b,c,d) for the hot/cold load vacuum setup together with the cryostat, where LO beam from the FIR gas laser is indicated, but the laser itself is not shown. Photo of our cryostat, including the mixer block, bias tee, circulator and LNA in (e).

Figure 1 shows the schematic of our heterodyne measurement setup for measuring the T_{rec}^{DSB} and G_m^{DSB} in (a), three photos on the THz part of the setup in (b-c), and a photo including the mixer block and the cold IF chain in the cryostat in (e). The LO is the far-Infrared (FIR) gas laser at 5.25 THz. A voice coil attenuator together with a proportional–integral–derivative (PID) feedback loop is used to sweep the LO power to determine T_{rec}^{DSB} or stabilize the power to measure IF NBW. The LO entered a blackbody hot (293 K)/cold (77K) vacuum unit attached to the 4 K cryostat via a window and then was reflected by a 6 μm Mylar beam splitter. The vacuum setup is to avoid the high air absorption loss at 5.25 THz. The combined radiation (LO + hot/cold loads) propagates to the lens-antenna coupled HEB mixer through a QMC multimesh low pass filter with a cut-off frequency of 5.8 THz. It acts as a heat filter and is referred as the "5.8 THz low pass filter" in Figure 1. The Si lens [25] used has an anti-reflection (AR) coating. But the AR was designed for 1.6 THz. The mixer is mounted on a metal block, which is fixed on the 4 K plate of the cryostat, but with a relatively poor

thermal interface. A heater together with a sensor is installed on the mixer block to elevate the local temperature of the mixer from 6.5 K to 23 K. The IF chain contains of a bias-T (0.2-18 GHz), a circulator (1.3-1.7 GHz), a cryogenic low noise amplifier (LNA#1, 0.1-14 GHz), where the circulator is dedicated to G_m^{DSB} measurements. All of cryogenic IF components are well contacted to the 4 K plate thermally. The room temperature part of the IF chain includes two LNAs (LNA#2: 0.1-14 GHz and LNA#3: 0.1-12 GHz), a band pass filter (BPF), a low pass filter (LPF), and a microwave power meter. The IF is filtered at 1.7 GHz by the BPF with a bandwidth of 85 MHz for T_{rec}^{DSB} and G_m^{DSB} measurements. Since the BPF is not capable of blocking the signals beyond 5 GHz, the LPF is added before the power meter. The IF chain has the total gain of 85 dB and the noise contribution of 4.7 K at 1.7 GHz.

The setup is also used for measuring IF NBW in the range of 0.2-14 GHz by removing the circulator, the BPF, the LNA#3, and the LPF, but replacing the power meter with a spectrum analyzer.

Table I summarizes the optical loss ($1/G_{opt}$) at 5.25 THz in the optical path from the hot/cold loads to the HEB, which includes the 6 μm thick Mylar beam splitter, the 5.8 THz low pas filter acting as a heat filter, the Si lens, and the power coupling from antenna to HEB. The Si lens used has an anti-reflection (AR) coating, designed for 1.6 THz. The optical loss of the AR coated Si lens is simulated using COMSOL Multiphysics by taking the absorption coefficients of Parylene-C of 27 cm^{-1} at 5.25 THz into consideration [26,27]. The power loss from antenna to HEB is estimated to be 0.94 dB due to the lower HEB impedance (51 Ω) and is 0.31 dB more than the matched case [22].

TABLE I. Loss of the components in the optical path from the hot/cold loads to the HEB at 5.25 THz, including the Mylar beam splitter (BS) (LBS) at 300 K, the 5.8 THz low pass filter (L_{filter}) at 4 K, the coated Si lens (L_{lens}) at 4 K, and the coupling between antenna and HEB. The measured T_{rec}^{DSB} together with an expected one if two components are optimized.

	L_{BS} (dB)	L_{filter} (dB)	L_{lens} (dB)	L_{coup} (dB)	T_{rec}^{DSB} (K)
6 μm BS & unoptimized coated lens	1.4	0.81	0.92	0.94	3960
3 μm BS & optimized coated lens	0.71	0.81	0.32	0.94	2920 (Estimated)

3. MEASUREMENT RESULTS

3.1 Current-voltage characteristics

Figure 2 shows a set of IV curves of the HEB from zero to fully pumped by the 5.3 THz LO, recorded at 20 K. Within the optimal operating region (2.5-4 mV and 0.19-0.25 mA), the T_{rec}^{DSB} of the HEB, to be described, only increases by ~5% from its lowest value. From the optimally pumped IV we derive the LO power of 9.5 μW at the HEB using the Isothermal technique [28], implying a power of ≤0.5 mW from the FIR laser. Such a power can be provided by THz quantum cascade lasers, e.g. 50 mW reported in [29].

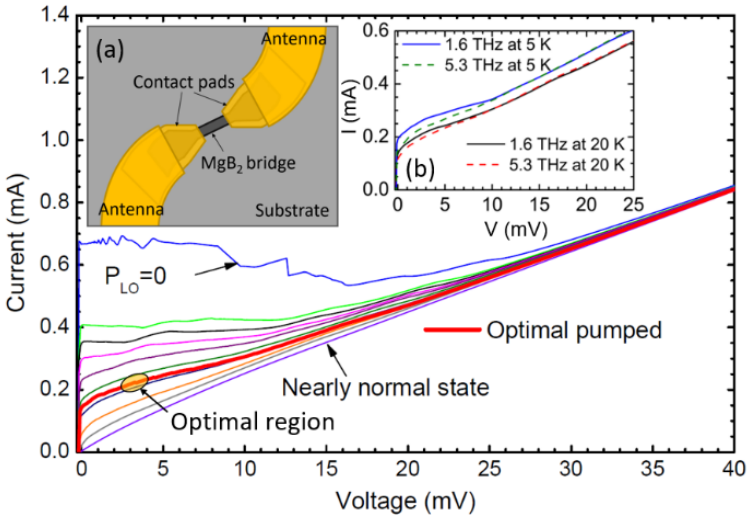

FIG. 2. A set of current-voltage (IV) curves of a MgB2 HEB mixer at 20 K by varying a 5.3 THz LO from zero to fully pumped to nearly normal state. The yellow circle indicates the optimal operating region for the lowest receiver noise temperature (≤5%). At this optimal IV, the required LO power is 9.5 μW. Inset (a) is an artistic impression of the HEB, which has the exactly same layout as the design; Inset (b) shows a comparison of the pumped IV curves with the same LO power at 1.6 THz and 5.3 THz, which are measured at 5 K and 20 K, respectively [19].

3.2 Receiver noise temperature and gain at 20 K and 6 K

A T_{rec}^{DSB} for the mixer is obtained by using the Y-factor technique. The receiver output powers responding to the hot (P_{hot}) and cold loads (P_{cold}) are measured, and the ratio between these two is the Y-factor. Combining the Y-factor and the Callen-Welton temperatures of the blackbody loads, a T_{rec}^{DSB} can be obtained [24]. The P_{hot} and P_{cold} are scanned as a function of HEB current at different DC biased voltages, where the current reflects the scan of LO power by the voice coil attenuator. In this way, the T_{rec}^{DSB} is not influenced by the fluctuations of the LO power and by the direct detection effect [2, 22]. The latter was negligible in our case because the required LO power (9.5 μW) is three orders of magnitude higher than the RF power (~10 nW) that is the difference between the hot and old loads. This is confirmed by the fact that we have not seen any shifts in pumped IV curves between two loads. Figure 3 plots the P_{hot} and P_{cold} as a function of current at the fixed bias voltage of 2.5 mV, measured at 20 K, and their polynomial fitted curves. The latter are used to determine the T_{rec}^{DSB}, plotted in the same figure, from which we select the minimum T_{rec}^{DSB}. We have carried out such measurements at a number of bias voltages ranging from 1 to 7 mV to obtain the minimum T_{rec}^{DSB} at each bias voltage. The results are summarized in the inset of Figure 3. The lowest T_{rec}^{DSB} is 3960 K when the HEB is biased at 2.5 mV and 0.21 mA.

The T_{rec}^{DSB} can be broken down to its constituents with the following standard expression [2]:

$$T_{rec}^{DSB} = T_{opt} + \frac{T_m^{DSB}}{G_{opt}} + \frac{T_{IF}}{G_{opt} G_m^{DSB}}, \quad (1)$$

$$T_m^{DSB} = \frac{T_{out}}{G_m^{DSB}}, \quad (2)$$

where $T_{opt}$is the noise temperature contribution of the optics ($= 137\ K$) and T_{IF} the noise temperature of the IF chain ($= 4.7\ K$). For simplicity, the contribution of the QN is not included in our broken-down analysis[28]. Furthermore, the $T_m^{DSB}$is determined by T_{out} and G_m^{DSB} through Eq. 2, from which we derive T_{out}.

The measured T_{rec}^{DSB}could be reduced to 2920 K if we would apply a Si lens with an AR coating optimized for 5.3 THz and utilize a thinner Mylar beam splitter of 3 μm. The detailed reduction values of optical loss can be found in Table I, which includes also both measured and expected T_{rec}^{DSB}.

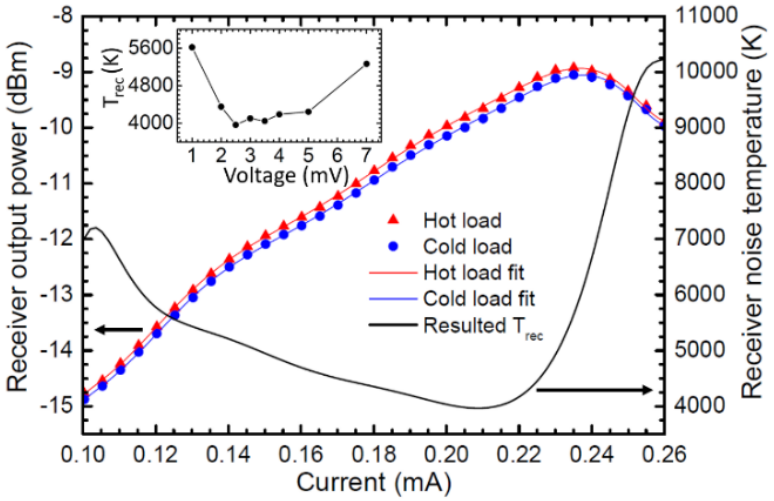

FIG. 3 Measured receiver output power (left axis) of the MgB_2HEB in response to hot/cold loads, together with the polynomial fits (in a solid line) as a function of the current and the resulted receiver noise temperature (right axis) when it is operated with an LO at 5.3 THz and at 20 K, and biased at 2.5 mV. The lowest noise temperature is 3960 K. The inset shows the minimum receiver noise temperature from such measurements for different bias voltages, varying from 1 to 7 mV [19].

At the optimal operating point where T_{rec}^{DSB} appears to be the lowest, the receiver conversion gain ($G_{rec}^{DSB} = G_{opt}G_m^{DSB}$) is measured by using the U-factor [30], which is the ratio between the receiver output power when the HEB is in its operating point and the receiver output power when it is in its superconducting state. The G_m^{DSB} is -7.6 dB by subtracting all the optical losses from the G_{rec}^{DSB} based on the measured U-factor of 14.3 dB. The T_m^{DSB} is 1470 K and the T_{out} is 250 K using Eqs. 1&2. We note that the circulator in our setup is crucial to obtain the reliable U-factor because it prevents the standing waves between the HEB and the LNA (see Figure 5(a)).

The T_{rec}^{DSB} of the same HEB was also measured at 6.5 K. We obtain a T_{rec}^{DSB} of 3530 K, resulting in a T_m^{DSB} of 1300 K, at the bias voltage of 2.5 mV, same as at 20 K, but at a slightly lower current (0.19 mA). Interestingly, the T_{rec}^{DSB} is only 12 % lower than the value at 20 K. The small difference between 6 K and 20 K should be attributed to the high T_c. The measured G_m^{DSB} is -6.7 dB at 6.5 K and is clearly higher than what was found (≤ -8.7 dB) from a NbN HEB at 5.3 THz at 4 K [8]. In contrast, the difference of T_{rec}^{DSB} between 5 K to 20 K was much larger and was 75 % for a HEB with a T_c of 31 K [15].

3.3 Temperature dependence of the mixer performance

To understand the origin of the slow increase of T_{rec}^{DSB} from 6 K to 20 K, we measured both T_{rec}^{DSB} and G_{rec}^{DSB} of the HEB fixed at the biasing point of 2.5 mV and 0.19 mA by varying the temperature from 6.5 to 22.5 K. To keep the same biasing point, the LO power has to be reduced with increasing the temperature by about 2 μW. Since we focus on the operating at 20 K, we discuss the data only up to this temperature. We find a very similar temperature dependence between T_{rec}^{DSB} and T_m^{DSB}(Figure 4), where there is an increase of 18 % for T_{rec}^{DSB} (between 6.5 K and 20 K), while 19 % for T_m^{DSB}. The ratio of the absolute value of the increase, 656 K for ΔT_{rec}^{DSB} and 249 K for ΔT_m^{DSB}, can be explained by the G_{opt} (-4.1 dB). However, both T_{rec}^{DSB} and T_m^{DSB} remain nearly constant below 10 K.

In essence, the temperature dependence of T_m^{DSB} originates from G_m^{DSB} and T_{out}, both of which decrease with increasing temperature, as shown in Figure 4. Furthermore, the G_m^{DSB} decreases faster than the T_{out}, leading to the increase of T_m^{DSB} with the temperature according to Eq. 2. Such temperature dependences are relatively unexplored experimentally although the dependence with the very limited number of data points was reported in [31]. In theory, one expects a decrease of T_{out} by increasing the operating temperature based on the hotspot model [32-34] because a bell-shaped electron temperature (T_e) profile along an HEB at a lower temperature becomes a flat one by increasing the

temperature up to T_c, but simultaneously decreasing LO power for the fixed bias point. The flat T_e profile results in a lower effective T_e in the center of the HEB, which in turn decreases T_{out} since T_{out} is dominated by the thermal fluctuation noise ($\propto T_e^2$). With regard to G_m^{DSB}, one also expects it to decrease with increasing the temperature because of the T_e profile and the reduced LO power. The behavior in our case is qualitatively in line with the simulation reported in [34]. It would be really useful if one can run a numerical simulation to explain quantitatively the temperature dependence of G_m^{DSB} and T_{out}.

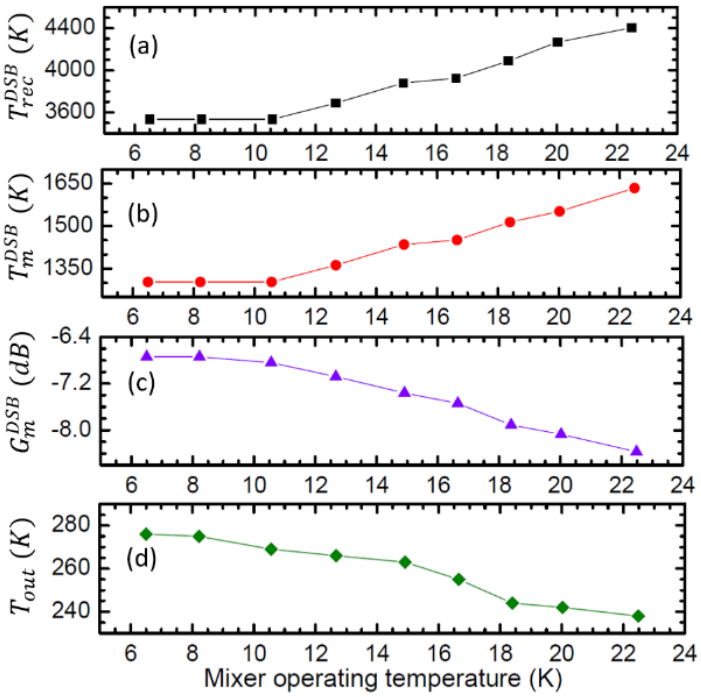

FIG. 4. Measured receiver noise temperature T_{rec}^{DSB} (at 1.7 GHz) in (a), derived mixer noise temperature T_m^{DSB} in (b), measured mixer conversion gain G_m^{DSB} in (c), and derived output noise T_{out} in (d) of the MgB_2 HEB mixer as a function of operating temperature [19].

3.4 IF noise bandwidth

The IF NBW of the HEB can be obtained from T_{rec}^{DSB} measurements in a wide IF range. Figure 5 (a) shows the P_{hot} and P_{cold} measured at 5.3 THz over an IF range of 0.2-14 GHz, from which the T_{rec}^{DSB} is derived and plotted as a function of IF in Figure 5 (b). The equation, $T_{rec}^{DSB}(f) = T_0(1 + (f/NBW)^2)$, is used to fit the T_{rec}^{DSB} data to obtain an NBW, which is 9.5 GHz $\pm$ 1GHz. We believe the low signal-to-noise ratio at the IF can affect the absolute value. As a confirmation, we find the NBW of 11 GHz $\pm$ 1GHz of the same HEB at 1.6 THz LO and at 5 K, which agrees to the reported result [15]. The large fluctuations of P_{hot} and P_{cold}, highlighted around 8 GHz in an inset in (a), result in the larger peak/dip in (b), which is believed to be a technical issue in the IF chain, but not from the HEB.

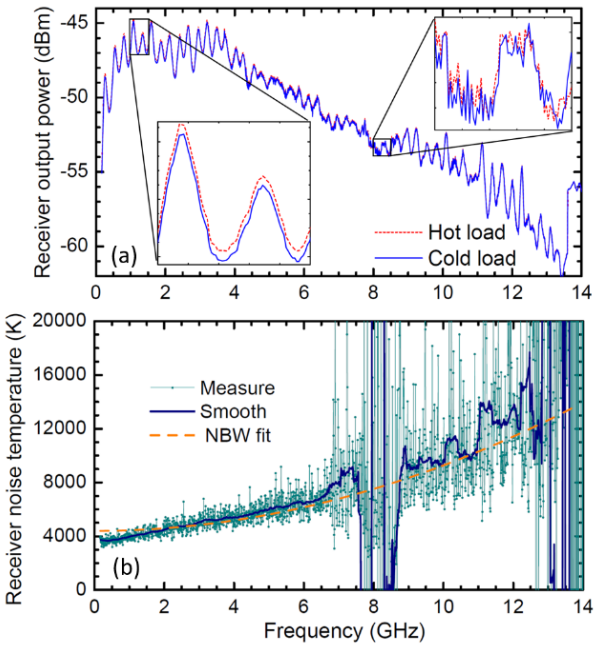

FIG. 5. (a) Measured receiver output powers of the MgB2 HEB at 5.3 THz, corresponding to hot and cold loads as a function of Intermediate frequency (IF) when it is in its optimal operating point and at 20 K. The inset zooms in the frequency range of 1-1.5 GHz and 8-8.5 GHz; (b) Receiver noise temperature as a function of IF. The orange line is the best fit of $T_{rec}^{DSB}(f) = T_0(1 + (f/NBW)^2)$ to the data, where the NBW, noise bandwidth, is 9.5 GHz [19].

3.5 Double-gap effect in MgB_2

MgB_2 is known to have two families of conduction bands with distinct superconducting gaps [35], π-band Δ_π and σ-band Δ_σ. The π-band Δ_π=1.8 meV and σ-band Δ_σ=6.3 meV of MgB_2 were reported for a T_c of 38.7 K [35], corresponding to the gap frequency of 0.87 THz and 3.05 THz, respectively. Assuming these two gap frequencies apply also to our HEB since the T_c of our MgB_2 film is 38.4 K and is nearly the same as in [34], one would expect a different pumped IV when it is at 5.3 THz, where the THz photons can break all the Cooper-pairs and can be uniformly absorbed within the thin, narrow MgB_2 bridge, however, when it is at 1.6 THz, the photons can break the Cooper-pairs in the π-band and only those in σ-band, which locate in the middle of the bridge and have a relative high temperature when DC heat power is present, and the photons thus can be non-uniformly absorbed. Inset (b) in Figure 2 shows pumped IV curves at 1.6 THz and 5.3 THz measured at 5 K and 20 K, respectively, where the IV at 5.3 THz has a lower current than that at 1.6 THz at the low bias voltages. This effect, as one would expect, is stronger at 5 K, while the two IV curves are exactly the same at the high voltages. The latter suggests that the pumped LO power is the same. The effect is analogous to the NbN HEB operated below and above its gap frequency, where the IV curves at two LO frequencies differ at low voltages [36]. In addition, the G_m^{DSB}at 1.6 THz is found to be slightly lower than that at 5.3 THz, which may further support that the double-gap effect plays a role in our experiment. Interestingly, this experiment implies that to explain the RF performance of a MgB_2 HEB, one needs to be aware of the operating frequency with respect to the two gap frequencies.

4. DISCUSSIONS

The measured T_{rec}^{DSB} could increase by less than 2 % and thus remain nearly unchanged if the LNA is also operated at 20 K instead of 4 K in our current measurement, where T_{IF} will increase from 4.7 K to 8.9 K. This discussion is motivated by the fact that, if the HEB is operated at 20 K using a Stirling cooler[17], then the LNA will also be at the same operating temperature. On the other hand, negligible effect to the measured T_{rec}^{DSB} by raising the operating temperature

of the LNA is expected since our MgB_2 HEB mixer has a T_{out} of 250 K, being much (a factor of 28) higher than the T_{IF}. In other words, the T_{rec}^{DSB} for the MgB_2 HEB is much less affected by the noise temperature of a LNA.

The sensitive MgB_2 HEB mixer with a large NBW, which can be operated at 20 K in a Stirling cooler, is promising for space applications. Based on the measured 3960 K, the expected, lowest T_{rec}^{DSB} of 2720 K at 5.3 THz by using the optimized coating lens (→3470 K), the thinner beam splitter (→2920 K), and also the antenna matched HEB resistance (→2720 K), is 28 times lower than a Schottky diode mixer at 4.7 THz [37], but is only ~2.5 times more than an NbN HEB mixer at 5.3 THz [22].

5. CONCLUSIONS

In conclusion, we have demonstrated for the first time a low noise MgB_2 HEB mixer operated at 5.3 THz LO and at 20 K. The measurements give a receiver noise temperature T_{rec}^{DSB} of 3960 K, a mixer noise temperature T_m^{DSB} of 1470 K, and a mixer gain G_m^{DSB} of -7.6 dB. The mixer can also be operated at a lower temperature. The measurements at 6.5 K or below give a T_{rec}^{DSB} of 3530 K, a T_m^{DSB} of 1300 K, and a G_m^{DSB} of -6.7 dB. The T_{rec}^{DSB} has a weak temperature dependence because of the high T_c, and has only 11-12 % decrease in the optimal value when the temperature changes from 20 K to 6.5 K or below. The measured IF noise bandwidth NBW is about 10 GHz at 5.3 THz and at 20 K. Additionally, we observed different IV curves at the low bias voltages, pumped at 1.6 and 5.3 THz, respectively, suggesting the presence of the two superconducting gaps in the ultra-thin MgB_2, which have never been observed before.

Acknowledgement

We thank J. Chang and F. van der Tak for their supports to this work, P. Khosropanah and A. Aminaei for their inputs on IF circuitry, and W. Laauwen, W-J. Vreeling, B. Kramer, H. Ode, and R.C. Horsten for their valuable technical supports. The work at Chalmers University of Technology was supported by Swedish Research Council (2019-04345) and Swedish National Space Agency (198/16). The work at TU Delft is partly supported by TU Delft Space Institute (DSI). Y. Gan is funded partly by the China Scholarship Council (CSC) and partly by the University of Groningen.

REFERENCES

[1] Gershenzon, E. M., Gol'tsman, G. N., Gogidze, I. G., Gusev, Y. P., Elant'ev, A .I., Karasik, B. S., and Semenov, A. D., "Millimeter and submillimeter range mixer based on electron heating of superconducting films in the resistive state," Sov. Phys. Supercond. **3**, 1582 (1990).

[2] Hubers, H.-W., "Terahertz Heterodyne Receivers," IEEE J. Sel. Top. Quantum Electron. **14**, 378 (2008).

[3] van der Tak, F. F. S., Madden, S. C., Roelfsema, P., Armus, L., Baes, M., Bernard-Salas, J., Bolatto, A., Bontemps, S., Bot, C., Bradford, C. M., Braine, J., Ciesla, L., Clements, D., Cormier, D., Fernandez-Ontiveros, J. A., Galliano, F., Giard, M., Gomez, H., Gonzalez-Alfonso, E., ... Spinoglio, L. "Probing the Baryon Cycle of Galaxies with SPICA Mid- and Far-Infrared Observations," Publ. Astron. Soc. Aust. **35**, e002 (2018).

[4] Risacher, C., Gusten, R., Stutzki, J., Hubers, Heinz-Wilhelm, Buchel, D., Graf, U., Heyminck, S., Honingh, C. E., Jacobs, K., Klein, B., Klein, T., Leinz, C., Putz, P., Reyes, N., Ricken, O., Wunsch, H.-J., Fusco, P., and Rosner, S., "First Supra-THz Heterodyne Array Receivers for Astronomy With the SOFIA Observatory," IEEE Trans. Terahertz Sci. Technol. **6**, 199 (2016).

[5] Hayton, D.J., Kloosterman, J.L., Ren, Y. , Kao, T.Y. , Hovenier, J.N. , Gao, J.R. , Klapwijk, T.M. , Hu, Q. , Walker, C.K. , Reno, J.L.,"A 4.7 THz Heterodyne Receiver for a Balloon Borne Telescope," Proc. SPIE **9153**, 91531R-1 (2014).

[6] de Graauw, T. Helmich, F.P. · Phillips, T.G. · Stutzki, J. Caux, E. Whyborn, N.D. et al, "The Herschel-Heterodyne Instrument for the Far-Infrared (HIFI)," Astron. Astrophys. **518**, 1 (2010).

[7] Kloosterman, J. L., Hayton, D. J., Ren, Y., Kao, T. Y., Hovenier, J. N., Gao, J. R., Klapwijk, T. M., Hu, Q.,. Walker, C. K., & Reno, J. L., "Hot electron bolometer heterodyne receiver with a 4.7-THz quantum cascade laser as a local oscillator," Appl. Phys. Lett. **102**, 011123 (2013).

[8] Zhang, W., Khosropanah, P., Gao, J.R., Kollberg, E.L., Yngvesson, K.S., Bansal, T., Barends, R., Klapwijk, T.M., "Quantum noise in a terahertz hot electron bolometer mixer," Appl. Phys. Lett. **96**, 111113 (2010).

[9] Linz, H., Beuther, H., Gerin, M., Goicoechea, J. R., Helmich, F., Krause, O., Liu, Y., Molinari, S., Ossenkopf-Okada, V., Pineda, J., Sauvage, M, Schinnerer, van der Tak, E. F. et al "Bringing high spatial resolution to the far-infrared," Exp. Astron. **51**:661-697 (2021).
[10] Waters, J.W. et al, "The Earth Observing System Microwave Limb Sounder (EOS MLS) on the Aura satellite," IEEE Trans. Geosci. Remote Sens. **44**, 1075 (2006).
[11] Canfield, P., and Crabtree, G., "Magnesium Diboride: Better Late than Never," Physics Today **56**, 34 (2003).
[12] Cherednichenko, S., Drakinskiy, V., Ueda, K., Naito, M., "Terahertz mixing in MgB2 microbolometers," Appl. Phys. Lett. **90**, 023507 (2007).
[13] Cunnane, D., Kawamura, J. H., Wolak, M. A., Acharya, N., Tan, T., Xi, X. X., Karasik, B. S., "Characterization of MgB_2 Superconducting Hot Electron Bolometers," IEEE Trans. Appl. Supercond. **25**, 2300206 (2015).
[14] Cunnane, D., Kawamura, J. H., Wolak, M. A., Acharya, N., Tan, T., Xi, X. X., Karasik, B. S., "Optimization of Parameters of MgB2 Hot-Electron Bolometers," IEEE Trans. Appl. Supercond. **27**, 1 (2017).
[15] Novoselov, E. and Cherednichenko, S., "Low noise terahertz MgB2 hot-electron bolometer mixers with an 11 GHz bandwidth," Appl. Phys. Lett. **110**, 032601 (2017).
[16] Acharya, N., Novoselov, E. and Cherednichenko, S., IEEE Trans. Terahertz Sci. Technol. **9**, 565 (2019).
[17] Aminou, D. M. A., Bézy, J.L., Meynart, Blythe, R., Kraft, P., S., Zayer, I., Linder, M., Falkner, M. and Luhmann, H.J., "Meteosat Third Generation (MTG) critical technology pre-development activities," Proc. SPIE **7474**, 747407 (2009).
[18] Karasik, B. S., a talk at EUCAS 2021, Moscow (unpublished)
[19] Gan, Y., Mirzaei, B., Silva, J. R. G. D., Chang, J., Cherednichenko, S., *van* der Tak, F., *and* Gao, J. R. "Low noise MgB_2 hot electron bolometer mixer operated at 5.3 THz and at 20 K," Appl. Phys. Lett. **119,** 202601 (2021).
[20] Novoselov, E., Zhang, N. and Cherednichenko, S.,"Study of MgB2 Ultrathin Films in Submicron Size Bridges," IEEE Trans. Appl. Supercond. **27**, 1 (2017).
[21] Focardi, P. Neto, A. McGrath, W. R, "Coplanar-waveguide-based terahertz hot-electron-bolometer mixers mproved embedding circuit description," IEEE Trans. Microw. Theory Tech. **50**, 2374 (2002).
[22] Zhang, W., Khosropanah, P., Gao, J. R., Bansal, T., Klapwijk T. M.,. Miao, W., and Shi, S. C, "Noise temperature and beam pattern of an NbN hot electron bolometer mixer at 5.25 THz," J. Appl. Phys. **108**, 093102 (2010).
[23] Kollberg, E.L., Yngvesson, K. S., Ren, Zhang, Y., W., Khosropanah, P. and Gao, J.R.,"Impedance of Hot-Electron Bolometer Mixers at Terahertz Frequencies" IEEE Trans. Terahertz Sci. Technol **1**, 383 (2011). The operating frequency of 5.3 THz is much higher than the two gap frequencies (0.87 and 3.05 THz described in section 3.5). The skin depth in our case is 75 nm, which is about 25 % of the width. So, we expect the current along the direction of the width to be constant, based on the calculation in Figure 5 in this paper although it is for NbN HEB.
[24] Khosropanah, P, Gao, J. R., Laauwen, W. M., Hajenius, M., and Klapwijk, T. M., "Low noise NbN hot electron bolometer mixer at 4.3 THz," Appl. Phys. Lett. **91**, 221111 (2007).
[25] We use an elliptical Si lens with the semi-minor axis of the ellipse *a* of 5 mm, the semi-major axis *b* of 5.235 mm, and the extension *c* from geometric center of the lens of 1.2 mm thick Si and 0.32 mm thick SiC substrate. This combination forms a nearly perfect elliptical lens based on the simulation by COMSOL Multiphysics. The refractive index is 3.38 for Si and 3.14 for SiC.
[26] Gan, Y. , Mirzaei, B. , van der Poel, S. , Silva, J.R.G. , Finkel, M. , Eggens, M. , Ridder, M. , Khalatpour, A. , Hu, Q., van der Tak, F Y. and Gao, J.R., "3.9 THz spatial filter based on a back-to-back Si-lens system," Opt. Express **28**, 32693 (2020).
[27] Gatesman, A. J. , Waldman, J. , Ji, M. , Musante, C. , Yagvesson, S., "An Anti-Reflection Coating for Silicon Optics at Terahertz Frequencies," IEEE Microwave and Guided Wave Letters **10,** 264 (2000).
[28] Ekström, H., Karasik, B. S., Kollberg, E.L., Yngvesson, K. S.,, "Conversion gain and noise of niobium superconducting hot-electron-mixers"IEEE Trans Microw. Theory Tech. **43,** 938 (1995).
[29] Khalatpour, A., Reno, J.L., and Hu, Q., "Phase-locked photonic wire lasers by π coupling," Nat. Photonics **13**, 47 (2019).
[30] Cherednichenko S, Kroug M, Merkel H, Khosropanah P, Adam. A, Kollberg E, Loudkov D, Gol'tsman G, Voronov B, Richter. H, and Huebers, H., "1.6 THz HEB mixer for far infrared space telescope (Hershel)," Phys. C: Supercond. and Its Applicat. **372–376**, 427 (2002).

[31] Novoselov, E. and Cherednichenko, S., "Gain and Noise in THz MgB2 Hot-Electron Bolometer Mixers With a 30-K Critical Temperature" IEEE Trans. Terahertz Sci. Technol. **7**, 704 (2017).
[32] Wilms Floet D., Miedema E., Klapwijk T.M., Gao J.R., "Hotspot mixing: A framework for heterodyne mixing in superconducting hot-electron bolometers," Appl. Phys. Lett. **74**, 433 (1999).
[33] Merkel, H. F., Khosropanah, P., Wilms Floet, D., Yagoubov, P. A., and Kollberg, E. L., "Conversion gain and fluctuation noise of phonon-cooled hot-electron bolometers in hot-spot regime," IEEE Trans. Microwave Theory Tech. **48**, 690 (2000).
[34] Miao, W., Zhang, W., Zhou, K. M., Gao, H., Zhang, K., Duan, W. Y., Yao, Q. J., Shi, S. C., Delorme, Y., and Lefevre, R., "Investigation of the Performance of NbN Superconducting HEB Mixers of Different Critical Temperatures," IEEE Trans. Appl. Supercond. **27**, 1 (2017).
[35] Putti, M., Affronte, M., Ferdeghini, Manfrinetti, P., C., Tarantini, C., and Lehmann, E., "Observation of the Crossover from Two-Gap to Single-Gap Superconductivity through Specific Heat Measurements in Neutron-Irradiated MgB2," Phys. Rev. Lett. **96**, 077003 (2006).
[36] Miao W., Zhang W., Zhong J.Q., Shi S.C., Delorme Y., Lefevre R., Feret A., "Non-uniform absorption of terahertz radiation on superconducting hot electron bolometer microbridges," Appl. Phys. Lett. **104**, 052605 (2014).
[37] Mehdi, I., Siles, J. V., Lee, C., and Schlecht, E.,"THz Diode Technology: Status, Prospects, and Applications," Proc. IEEE **105**, 990 (2017).